Ligand Binding and Protein Dynamics in Cupredoxins†

David Ehrenstein,‡ Mattia Filiaci,‡ Birgit Scharf,§ Martin Engelhard,§ Peter J. Steinbach,|| and G. Ulrich Nienhaus*,‡

Department of Physics, University of Illinois at Urbana-Champaign, 1110 West Green Street, Urbana, Illinois 61801-3080, Max-Planck-Institut für molekulare Physiologie, Rheinlanddamm 201, 44139 Dortmund, Germany, and Division of Computer Research and Technology, Building 12A, National Institutes of Health, Bethesda, Maryland 20892-5626

Received February 22, 1995; Revised Manuscript Received May 18, 1995⊗

ABSTRACT: Type 1 copper sites bind nitric oxide (NO) in a photolabile complex. We have studied the NO binding properties of the type 1 copper sites in two cupredoxins, azurin and halocyanin, by measuring the temperature dependence of the ligand binding equilibria and the kinetics of the association reaction after photodissociation over a wide range of temperature (80−280 K) and time (10^{-6}−10^{2} s). In both proteins, we find nonexponential kinetics below 200 K that do not depend on the NO concentration. Consequently, this process is interpreted as geminate recombination. In azurin, the rebinding can be modeled with the Arrhenius law using a single pre-exponential factor of $10^{8.3}$ s^{-1} and a Gaussian distribution of enthalpy barriers centered at 22 kJ/mol with a width [full width at half-maximum (FWHM)] of 11 kJ/mol. In halocyanin, a more complex behavior is observed. About 97% of the rebinding population can also be characterized by a Gaussian distribution of enthalpy barriers at 12 kJ/mol with a width of 6.0 kJ/mol (FWHM). The pre-exponential of this population is 1.6×10^{12} s^{-1} at 100 K. After the majority population has rebound, a power-law phase that can be modeled with a γ-distribution of enthalpy barriers is observed. Between 120 and 180 K, an additional feature that can be interpreted as a relaxation of the barrier distribution toward higher barriers shows up in the kinetics. Above 200 K, a slower, exponential rebinding appears in both cupredoxins. Since the kinetics depend on the NO concentration, this process is identified as bimolecular rebinding. Structural aspects of the copper−NO complex are discussed. NO binding to cupredoxins shows interesting analogies to the ligand binding reaction in heme proteins. Thus, we conclude that the concepts regarding conformational heterogeneity and dynamics, which have been developed from heme protein experiments, are also applicable to proteins with different active sites and secondary structures.

Nitric oxide (NO) is a toxic free radical. The recent discovery that this molecule plays a key role in biological signal transduction and cytotoxicity has stimulated much research on the function of NO in living systems. Metal centers are involved in both the biological NO synthesis and signal transduction. Most studies have focused on iron in heme (guanylate cyclase and NO synthase) and non-heme proteins. Copper proteins are ubiquitous in living systems, and hence, it would not be a surprise if new physiological roles for copper−NO interactions beyond their well-established involvement in bacterial nitrification and denitrification functions would be discovered.

We have studied NO binding to cupredoxins, a class of small, mononuclear copper proteins involved in electron transfer reactions (Adman, 1985). They contain a single blue (type 1) copper site, which is characterized by a strong absorption band at ~600 nm that gives rise to the blue color and an electron paramagnetic resonance (EPR) spectrum with unusually small $A_{||}$ values (Solomon & Lowery, 1993). Crystal structures for a number of cupredoxins show that both the β-sandwich structure and the geometry of the copper site are highly conserved, regardless of their biological origin (Adman, 1991). The copper is coordinated to one cysteine sulfur and two histidines in a trigonal-planar environment with a weaker axial ligand (usually methionine) at a larger distance. The unusual spectral properties derive mainly from the interactions of the copper with the cysteine sulfur (Gray & Solomon, 1981; Sanders-Loehr, 1993; Solomon & Lowery, 1993).

Our ligand binding studies in cupredoxins were motivated by the desire to test and generalize the concepts of conformational heterogeneity and dynamics that were obtained from ligand binding reactions in heme proteins. These studies have contributed to our understanding of the relation between the structure, dynamics, and function of proteins (Austin et al., 1975; Steinbach et al., 1991). Sperm whale myoglobin (Mb), a small, globular heme protein of 17.8 kD, has served as a model system in these studies. Diatomic ligands (O_2 and CO) bind at the heme iron. An important concept was developed on the basis of the observation of nonexponential rebinding after photodissociation at low temperatures. Proteins do not exist in a unique, well-defined structure, but in a large number of slightly different structures, called conformational substates (CS). Evidence for CS comes also from the analysis of the Debye−Waller factor in protein crystals by X-ray diffraction (Frauenfelder et al., 1978; Hartmann et al., 1982; Parak et al., 1987) and from the inhomogeneity of spectral lines (Campbell et al., 1987; Ormos et al., 1990). The CS appear to be grouped in different tiers with distinctly different barrier heights between the substates, leading to a hierarchical model of the confor-

† This work was supported in part by the National Science Foundation (Grant DMB 87-16476), the National Institutes of Health (Grant GM 18051), and the University of Illinois at Urbana-Champaign. G.U.N. acknowledges fellowship support from the Center for Advanced Study, University of Illinois at Urbana-Champaign.

* Author to whom correspondence should be addressed.
‡ University of Illinois at Urbana-Champaign.
§ Max-Planck-Institut für molekulare Physiologie.
|| National Institutes of Health.

⊗ Abstract published in *Advance ACS Abstracts,* September 1, 1995.

0006-2960/95/0434-12170$09.00/0

mational energy landscape in MbCO (Ansari et al., 1985; Frauenfelder et al., 1994).

To study the generality of these concepts, we performed ligand binding experiments on two cupredoxins, azurin and halocyanin. Azurin (Az, from *Pseudomonas aeruginosa*) is a small blue copper protein that serves as an electron carrier in certain bacterial redox chains. It has a molecular weight of 14 600. Halocyanin (Ha) was discovered only recently (Scharf & Engelhard, 1993) and is one of the minority of known small blue copper proteins that is associated with the cell membrane, although probably not embedded in it (Mattar et al., 1994). It comes from the archaebacterium *Natronobacterium pharaonis*, which is found in the brines of the Wadi Natrun lakes of North Africa, where the salinity is 30% and the pH is around 11. Halocyanin is only the second blue copper protein discovered in the kingdom of archaebacteria (Scharf & Engelhard, 1993). Its existence in a separate kingdom suggests extremely early origins for the class, contrary to a conventional theory that they evolved from photosynthetic eubacteria (Mattar et al., 1994). Halocyanin is clearly a blue copper protein, on the basis of spectroscopic, biochemical, and primary sequence data, and therefore is assumed to be involved in electron transfer, although its redox partners are not yet identified. Circular dichroism (CD) spectroscopy and sequence analysis imply that Ha consists of at least 95% β-sheet structure. It contains the four copper ligands at roughly the same sequence positions as Az. Its molecular weight is also similar at 15 500. It is possible to fit the sequence into the X-ray structure of azurin (W. Mäntele, personal communication). The most distinguishing element of the Ha structure is the post-translational attachment of a lipid, which anchors it to the cell membrane.

Blue copper centers (type 1 copper) bind NO (Gorren et al., 1987). Upon binding, the strong absorption band at ~600 nm is bleached. The Cu−NO complex can be photodissociated, and the absorption band at ~600 nm that is responsible for the blue color reappears. We have previously published a study of NO binding to azurin (Ehrenstein & Nienhaus, 1992). Here, we report on the temperature dependence of the NO binding equilibrium and the binding kinetics after photodissociation in halocyanin. The large dynamic range of these experiments enables us to distinguish three different geminate recombination processes. We also discuss similarities between ligand binding processes in cupredoxins and heme proteins.

MATERIALS AND METHODS

Lyophilyzed azurin from *P. aeruginosa* was purchased from Sigma (St. Louis, MO) and used without further purification. The protein was dissolved in a mixture of 70% glycerol and 30% 0.1 M acetate buffer at pH 5.5 (v/v) to obtain a protein concentration of ~100 μM. Halocyanin was isolated from *N. pharaonis* as described by Scharf and Engelhard (1993). The stock of 5 mM protein in 100 mM phosphate buffer and 100 mM detergent was diluted to a final protein concentration of 300 μM with a mixture of 70% glycerol and 30% phosphate buffer at pH 7.

The NO incubation procedures were done at 0 °C. While the sample was stirred for 1 h, the atmosphere above the solution was replaced several times by N_2 gas. NO gas (pressure, 1 bar) was washed in pH 10 carbonate buffer to remove residual N_2O_4 and then exchanged for the N_2 above the sample. The solution was allowed to incubate for another hour and transferred anaerobically into a sealed cuvette and cooled to cryogenic temperatures.

Optical spectra were measured with an OLIS-Cary 14 spectrometer interfaced to an IBM PC/AT (On-Line Instrument Systems Inc., Jefferson, GA) with a resolution of 2 nm. A closed-cycle helium refrigerator (Helix Technology Corp., CTI Cryogenics Division, Waltham, MA) cooled the sample. The temperature of the sample was measured with a silicon diode sensor and adjusted with a digital controller (model DRC93C; Lake Shore Cryotronics Inc., Westerville, OH) in the range between 10 and 300 K. The rebinding kinetics were studied with a flash photolysis system that employs a 6 ns (FWHM) wide pulse from a frequency-doubled, Q-switched Nd-YAG laser (532 nm, 300 mJ) for the photolysis (model NY-61; Continuum, Santa Clara, CA). Rebinding was monitored with light from a tungsten lamp that passed through a monochromator set at 628 nm for azurin and 600 nm for halocyanin. The monitor beam intensity was kept low so as to yield a photolysis rate coefficient of less than 10^{-2} s^{-1}. The light intensity was measured with a photomultiplier tube (model R 928; Hamamatsu Corp., Middlesex, NJ) and digitized with a homemade logarithmic time-base digitizer (Wondertoy II) (Berendzen et al., 1989) from 1 μs to 100 s. The sample was kept in a storage cryostat (model 10-DT; Janis Research Co. Inc., Wilmington, MA) equipped with a digital temperature controller (model DRC82C; Lake Shore Cryotronics Inc., Westerville, OH). The kinetics data shown in Figures 3, 4, and 6 are averages of up to 50 individual measurements.

EXPERIMENTAL RESULTS AND DATA EVALUATION

Equilibrium Properties. When NO is added to a solution of azurin or halocyanin at room temperature, only minimal absorption changes occur. As the temperature is lowered, the strong (Cys)S $\rightarrow$ Cu($d_{x^2-y^2}$) charge transfer band near 600 nm continuously decreases in intensity. For AzNO, it practically disappears at 200 K, while for HaNO, there is still residual absorbance (Figure 1). The decrease of the band is accompanied by an increase of the absorbance on the blue side of the spectrum. An isosbestic point exists near 538 nm in AzNO and 520 nm in HaNO. After illumination of the sample below 200 K, the band near 600 nm reappears and subsequently decays again in the dark. These results have been explained by the formation of a photolabile Cu−NO complex (Gorren et al., 1987). We used the area of the 600 nm band to determine the temperature dependence of the equilibrium coefficient, $\Lambda(T)$, of the reaction,

$$\mathrm{Cu} + \mathrm{NO} \rightleftharpoons \mathrm{CuNO} \qquad (1)$$

We evaluated the changes in free energy ΔG, enthalpy ΔH, and entropy ΔS (for a standard state of 0.1 MPa NO pressure above the sample) from the equilibrium coefficient using the van't Hoff equation,

$$\Lambda(T) = \frac{[\mathrm{AzNO}]}{[\mathrm{Az}]} = \exp\left(-\frac{\Delta G}{RT}\right) = \exp\left(-\frac{\Delta H}{RT}\right)\exp\left(\frac{\Delta S}{R}\right) \qquad (2)$$

R is the universal gas constant and T the absolute temperature. The van't Hoff plot, $\Lambda(T)$ versus ($10^3/T$), in Figure 2

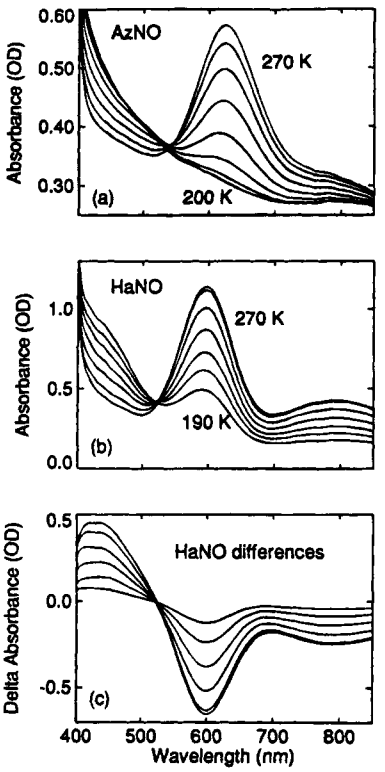

FIGURE 1: Equilibrium spectra of (a) AzNO and (b) HaNO as a function of temperature. (c) Difference spectra of HaNO obtained by subtracting each spectrum in (b) from the 190 K spectrum: $\Delta A(\lambda,T) = A(\lambda,190\ \mathrm{K}) - A(\lambda,T)$.

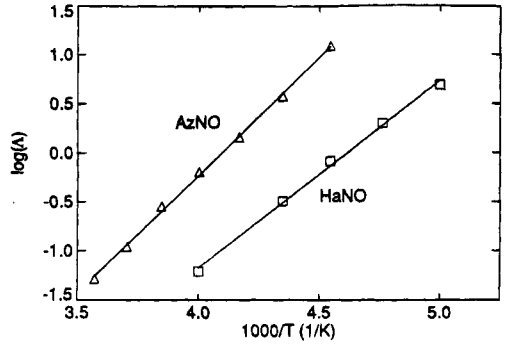

FIGURE 2: van't Hoff plot of the equilibrium coefficient $\Lambda(T)$ for the binding of NO to Az and Ha.

is linear, in agreement with eq 2, and yields $\Delta H = -(46 \pm 5)$ kJ/mol for AzNO and $\Delta H = -(37 \pm 5)$ kJ/mol for HaNO. These values are significantly less than typical heme protein values, so the Cu−NO bond is much weaker than the Fe−CO bond in heme proteins. For example, the binding enthalpy of CO to Mb is about −90 kJ/mol (Keyes et al., 1970; Austin et al., 1975). The plot also gives $\Delta S/R = -(23 \pm 3)$ for AzNO and $-(20 \pm 3)$ for HaNO. A typical heme protein value for $\Delta S/R$ is −14 (Frauenfelder & Wolynes, 1985). The lower binding entropies for Az and Ha imply that the bound state is significantly more restricted than it is in heme proteins.

Kinetic Experiments. Figure 3 shows the kinetics of NO binding to halocyanin after photodissociation. We plot the logarithm of the absorbance change after the photoflash, ΔA, versus log t. The absorbance change is taken to be proportional to the fraction of proteins, $N(t)$, that has not yet bound a ligand after time t. Below 200 K, we observe nonexponential kinetics (Figures 3a−c). Three different

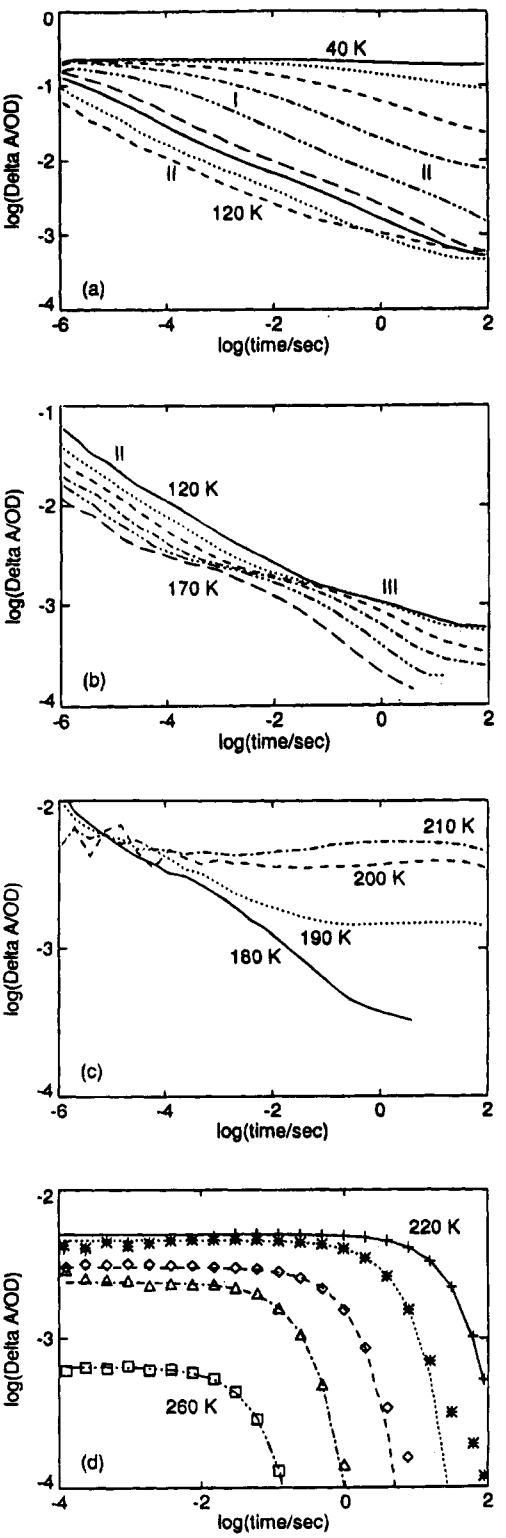

FIGURE 3: Flash photolysis kinetics of HaNO, 40−260 K, in 10 K steps, monitored at 600 nm. (a) Rebinding between 40 and 120 K, showing processes I and II. (b) Rebinding between 120 and 170 K, showing processes II and III. (c) Rebinding between 180 and 210 K, where the solvent process begins to appear. (d) Rebinding between 220 and 260 K, showing the exponential solvent process. Symbols: experimental data. Lines: curves obtained from fitting single exponentials, $N(t) = \exp(-t/\tau)$. The total amplitude decreases with increasing temperature because the equilibrium shifts toward the unligated species.

internally rebinding populations (I, II, and III) can be distinguished in HaNO and will be discussed in detail below. Above 200 K, another temporally well-separated process that

is close to exponential in time appears (Figure 3d), and its rate coefficient depends on the concentration of ligands in solution, which specifies this process as bimolecular recombination. Note that the total absorbance change, ΔA_{max}, decreases at the highest temperatures because of incomplete binding of NO, consistent with the data in Figure 2.

The overall kinetics of the HaNO recombination are similar to the kinetics of AzNO (Ehrenstein & Nienhaus, 1992) and the ligand binding to heme proteins and protoheme (Austin et al., 1975; Alberding et al., 1976; Miers et al., 1990; Steinbach et al., 1991). To describe the appearance of temporally well-separated geminate and bimolecular recombination, a kinetic scheme with at least three distinct kinetic states is necessary. For AzNO, we have shown that it is possible to adopt the scheme used in heme protein studies, where the states are represented by wells in a reaction enthalpy surface. In well A, the ligand is bound to the metal ion. In well B, the ligand is in the vicinity of the reactive site and has to surmount an enthalpy barrier, H_{BA}, to bind. In well S, the ligand is in the solvent and has to overcome two sequential barriers, H_{SB} and H_{BA}, to bind. The kinetics are governed by the four rate coefficients k_{BA}, k_{AB}, k_{BS}, and k_{SB}, where k_{SB} is a pseudo first-order rate coefficient in the presence of excess ligand. At temperatures below about 200 K, the ligand cannot escape from the protein after photodissociation ($k_{BS} = 0$) and rebinds internally (process I, B $\rightarrow$ A). At higher temperatures, the ligand either rebinds internally or escapes to the solvent. Subsequently, a ligand from the solvent binds to the protein (process S, S $\rightarrow$ B $\rightarrow$ A).

The nonexponential kinetics at temperatures below ~200 K, Figure 3 a–c, can be explained with the concept of conformational substates (CS). At low temperatures, the proteins are frozen into many CS with slightly different structures and activation enthalpies H_{BA} for ligand binding. In general, there will also be a distribution of activation entropies. However, only in cases where the enthalpy barriers are very low (e.g. protoheme–CO) does the distributed activation entropy affect the kinetics appreciably. If we assume that $k_{AB} \ll k_{BA}$, the fraction of proteins that have not yet rebound a ligand at time t after photodissociation is described by

$$N(t,T) \int g(H_{BA}) e^{-k_{BA}(H_{BA},T)t}\, dH_{BA} \qquad (3)$$

where the temperature dependence of the rate coefficient $k_{BA}(H_{BA},T)$ is usually given by the Arrhenius law,

$$k_{BA}(H_{BA},T) = A_{BA}(T/T_0) e^{-H_{BA}/RT} \qquad (4)$$

Here, A_{BA} is the pre-exponential, and T_0 is a reference temperature of 100 K.

Taking the measured absorbance change as proportional to $N(t,T)$, we have used eqs 3 and 4 to perform a nonlinear least-squares fit to the low-temperature data. For population I (Figure 3a), the kinetics at the various temperatures are fitted simultaneously with a single, temperature independent $g(H_{BA})$. We tried different model functions for $g(H_{BA})$ (Steinbach et al., 1992), but the Gaussian gave clearly the best fit. Figure 4 shows the rebinding data for HaNO between 40 and 80 K, monitored at 600 nm, together with the fitted kinetics shown as lines. The Gaussian enthalpy

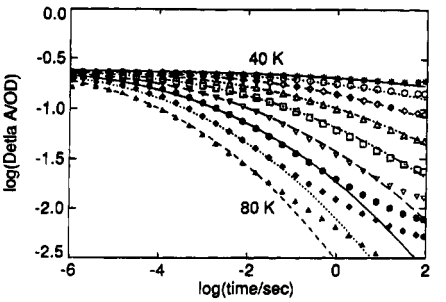

FIGURE 4: Data and $g(H)$ fits of HaNO kinetics, 40–80 K. Symbols: rebinding data for HaNO, 40–80 K, in steps of 5 K. Curves: fits to the data using eqs 3 and 4 with a Gaussian $g(H)$ distribution. The fits systematically miss below log $\Delta A = -2$ as process II sets in.

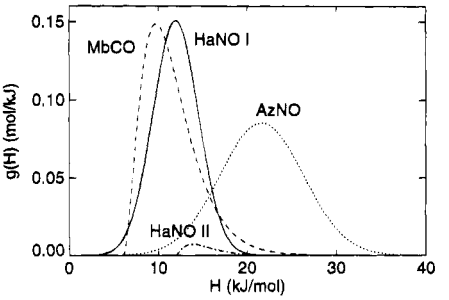

FIGURE 5: Activation enthalpy distributions from the low-temperature data of MbCO, HaNO, and AzNO. Pre-exponential values, $\log(A_{BA}/s^{-1})$, are 8.8 (MbCO), 12.2 (HaNO I), 9.2 (HaNO II), and 8.3 (AzNO).

Table 1: Parameters Determined from the $g(H)$ Fits to Flash Photolysis Kinetics

system	$\log(A_{BA}/s^{-1})$	H_{min} (kJ/mol)	H_{peak} (kJ/mol)	α^a
HaNO I	12.2		12.0	6.7
HaNO II	8.9	12.0	13.8	0.68
AzNO	8.3		21.6	11.0
MbCO	8.8	6.0	9.8	0.56

[a] The parameter α refers to the FWHM for Gaussian fits and to the width parameter for the γ-distribution, eq 4.

distribution $g(H_{BA})$ for HaNO is plotted in Figure 5 together with those of AzNO (measured at 628 nm) and MbCO (measured in the Soret band at 440 nm). Fit parameters are summarized in Table 1.

For temperatures above ~65 K, the fits in Figure 4 deviate markedly from the theoretical curves at longer times, indicating that another kinetic process (process II) appears. It is visible at the same vertical position ($\log(\Delta A) \approx -2$) over a range of at least 50 K, corresponding to about 3% of the total population. It continues through all higher temperatures as long as geminate rebinding is observed. The kinetics of process II have a very different shape from those of process I. The traces are quite straight on the log–log plot, which signifies a power-law time dependence and an enthalpy distribution with an exponential tail. A normalized γ-distribution (Young & Bowne, 1984),

$$g(H) = \frac{\alpha^{\alpha(H_{peak}-H_{min})+1}}{\Gamma(\alpha(H_{peak}-H_{min})+1)} \times (H-H_{min})^{\alpha(H_{peak}-H_{min})} e^{-\alpha(H-H_{min})} \qquad (5)$$

was fitted to process II (Figure 6) in a global fit using a

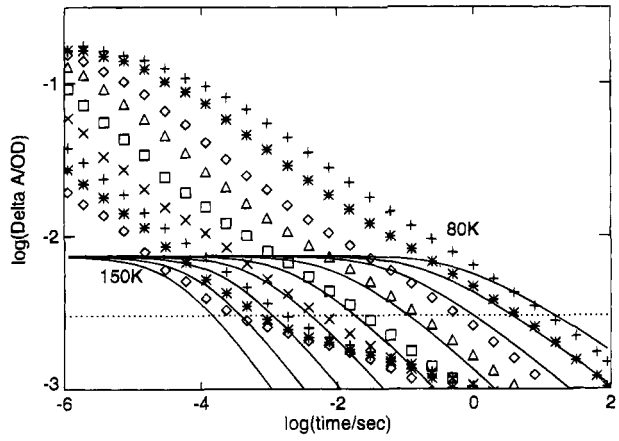

FIGURE 6: Fit of a γ-distribution to process II in HaNO. Symbols: flash photolysis data for HaNO, 80, 85, 90−150 K (in steps of 10 K.) Curves: fits to the data using eqs 3 and 4 with a γ-distribution, eq 5, (solid line) shown in Figure 5. Data below the horizontal line were ignored by the fit.

Gaussian distribution for process I. The γ-distribution turns on at H_{min} ($g(H \leq H_{min}) = 0$), reaches its maximum value at $H = H_{peak}$, and decays exponentially to 0. The fit parameters are included in Table 1.

At 120 K, another process appears after about 0.1 s (process III). In contrast to process II, this process increases in amplitude as temperature increases (Figure 3b). Thus, process III is not associated with a fixed fraction of the population. There are two physically quite different scenarios that can give rise to such a behavior. (1) A second geminate state B′ exists that is separated from B by an enthalpy barrier, which can be overcome more easily at higher temperatures, so that the amplitude of the B′ → A recombination increases with temperature. (2) The enthalpy barrier between B and A increases with time due to a protein relaxation (Steinbach et al., 1991). As we will describe below, there is evidence that the geometry of the copper site is altered substantially upon NO binding, transforming the distorted tetrahedral copper ligand geometry into a roughly square-planar arrangement. From our experience with Mb, we would expect the protein to relax back to its NO-free structure after photodissociation if sufficient thermal energy is available. Additional support for relaxation in HaNO comes from the fact that process I rebinds more slowly above 100 K than expected from the low-temperature fit in Figure 4. In addition to the geminate processes, the familiar bimolecular ligand binding process from the solvent sets in (Figure 3c,d) above 180 K.

DISCUSSION

Active Site Structure. When the copper is replaced by another metal ion or even removed, the ligating amino acids undergo very little structural rearrangement (Garrett et al., 1984; Shepard et al., 1990; Nar et al., 1992), implying that the protein imposes a rigid trigonal coordination geometry on the metal site (Williams, 1971; Gray & Malmström, 1983). A recent comparison of a series of cupredoxins showed that the electronic and EPR spectra reveal insights into the geometry of the copper site (Han et al., 1993; Romero et al., 1993; Lu et al., 1993). It was shown that not only the 600 but also the 460 nm band exhibits substantial (Cys)S → Cu(II) charge transfer character. Sites where the Cu is close to the trigonal ligand plane have a weak absorption at 460 nm, and the ratio of the extinction coefficients $R = \epsilon_{460}/\epsilon_{600} < 0.1$. By contrast, tetrahedrally distorted type 1 sites, where the Cu has moved toward the axial ligand, are characterized by an increased absorption at 460 nm, with $0.2 < R < 1.3$. In azurin, $R = 0.04$ (den Blaauwen et al., 1993), indicating that the copper is close to the trigonal ligand plane. X-ray structure analysis yields an out-of-plane displacement of 0.1 Å (Sykes, 1991). Halocyanin has $R \approx 0.15$, which is indicative of a larger tetrahedral distortion compared with azurin.

In which way does the copper site geometry change upon NO binding? When Gorren et al. (1987) observed the NO binding to Az, they suggested that it formed a charge transfer complex, Cu^+-NO^+, partly based on their observation of bleaching of the main absorption bands, which is also observed in reduction of the copper. However, the azurin spectra in Figure 1a show an isosbestic point at ~530 nm and increasing absorbance below that wavelength, indicating that a band appears around 400 nm, which does not exist in reduced Az (Corin & Gould, 1989). Halocyanin shows the same behavior, as evident from the spectra in Figure 1b,c. In fact, a band near 400 nm appears in all of the examples of NO binding to blue copper (Wever et al., 1973; van Leeuwen et al., 1975; van Leeuwen & van Gelder, 1978; Martin et al., 1981; Suzuki et al., 1989). On the basis of the optical spectra, we proposed earlier that a tetragonal Cu(II) complex is formed upon NO binding to azurin, with the copper residing in the plane formed by the two histidines, the cysteine, and the NO ligand (Ehrenstein & Nienhaus, 1992). Recent experiments using site-directed mutagenesis indeed support this scenario. They revealed that, when one of the three planar ligands is substituted by other amino acids, the copper site becomes more flexible and can accommodate up to four ligands in a square-planar geometry (den Blaauwen et al., 1991, 1993; Mizoguchi et al., 1992).

den Blaauwen et al. (1993) studied a mutant Az (His117Gly), where the solvent-accessible histidine that ligates the copper is replaced by a glycine, leaving the copper with direct access to the solvent. Using EPR, resonance Raman, and optical spectroscopies, they showed that various exogenous ligands, for example, imidazole, azide, and even water, can bind at the vacant copper coordination and recreate the characteristic properties of a blue copper site. Histidine or histamine can act as a bidentate ligand and cause the formerly tetrahedral binding geometry of the copper to change to a tetragonal, roughly square-planar geometry, with properties typical of type 2 copper sites. In each of their examples, den Blaauwen et al. observed an absorbance peak near 400 nm when the tetragonal site was formed, along with a bleaching of the typical blue copper absorption bands. They attributed the lack of the 460 and 630 nm charge transfer bands to a lengthening of the (Cys)S−Cu(II) bond as the copper moves into the plane of four ligands. We observe similar spectral changes upon NO binding. Apparently, NO as a strong ligand is capable of causing the same rearrangement in the native protein. Recent EXAFS data on Az mutants also indicate that the active site structure is flexible enough to be perturbed by changes in the copper ligands (Murphy et al., 1993).

The nonexponential kinetics in processes I and II imply structural heterogeneity of the active site. Process III may be the result of a relaxation of the copper out of the N−N−S plane toward the methionine sulfur and toward a more normal

blue copper structure, with concomitant increase of the rebinding barrier. This scenario would be analogous to the Mb* → Mb relaxation in MbCO (Steinbach et al., 1991; Nienhaus et al., 1992). In AzNO, we have not observed such a relaxation. A possible explanation is based on the differences in the copper site structures of Az and Ha. The copper in Az is fairly close to the N−N−S plane, compared with other blue copper proteins whose structures are available (Sanders-Loehr, 1993). The R value of halocyanin implies a larger tetrahedral distortion, with the copper farther away from the trigonal ligand plane in the native form. Thus after photolysis, the copper in Az may require less readjustment to return to the native state and hence does not show relaxation.

Ligand Binding in Proteins. The most extensive studies of ligand binding in proteins over wide ranges of time and temperature have been done on heme proteins. With the present work, we have extended these experiments to copper-containing proteins. Cupredoxins appeared particularly interesting to us because they are electron transfer proteins, and it had been suggested that they might have less conformational heterogeneity than other proteins because they depend on minimizing structural changes between oxidized and reduced states for efficient operation. We were also interested in observing the effects of β-sheet structures, since myoglobin and hemoglobin are made of α-helices. The lack of a heme group, which is connected with most of the heme protein spectral markers, could also conceivably have led to different results. But all of the kinetics in cupredoxins are surprisingly similar to those in heme proteins. Both geminate and bimolecular rebinding processes occur. The geminate rebinding is governed by distributions of enthalpy barriers (Figure 5).

In MbCO, the enthalpy distribution is asymmetric and can be described with a γ-distribution (Young & Bowne, 1984). The asymmetry arises mainly from the fact that MbCO has three taxonomic substates, denoted A_0, A_1, and A_3 (Mourant et al., 1993). They have different pre-exponentials and enthalpy barrier distributions, as determined by flash photolysis with monitoring in the infrared spectrum (Young et al., 1991). We have shown that the low-temperature rebinding kinetics of MbCO, measured in the visible spectrum, is consistent with a sum of Gaussian distributions of the three A substates (Steinbach et al., 1992). Temperature-derivative spectroscopy in the infrared spectrum at low temperatures also yields Gaussian enthalpy distributions for the individual A substates (Berendzen & Braunstein, 1990; Mourant et al., 1993). The barrier distribution for AzNO is Gaussian (Ehrenstein & Nienhaus, 1992), as is the distribution for the majority (97%) of the HaNO sample. A number of models have been proposed to explain the shapes of the $g(H_{BA})$ distributions. In these models, a protein coordinate, which represents the conformational heterogeneity, is coupled to the reaction coordinate. Depending on the assumptions about the shape of the conformational distribution and the nature of the coupling, one arrives either at a symmetric (Gaussian) (Agmon & Hopfield, 1983; Stein, 1985) or asymmetric $g(H_{BA})$ distribution (Young & Bowne, 1984; Šrajer et al., 1988). Our results with MbCO and AzNO suggested that the low-temperature enthalpy distributions may be intrinsically symmetric and Gaussian. In HaNO, the majority population fits nicely into this picture; the minority population II, however, rebinds with power-law kinetics and not with a Gaussian barrier distribution.

It is interesting to compare the pre-exponential factors, A_{BA}, for ligand binding to heme proteins and cupredoxins. The pre-exponential can be written as the product of a frequency factor, ν, and an entropy term, $\exp(S/R)$, where S is the activation entropy (Frauenfelder & Wolynes, 1985). For adiabatic reactions, the frequency factor is usually taken to be about 10^{12} s^{-1}. Pre-exponentials around 10^9 s^{-1} have been reported for rebinding of CO and O_2 in heme proteins (Steinbach et al., 1991). Frauenfelder and Wolynes (1985) have pointed out that the low pre-exponentials can be explained by a substantial entropy reduction when the ligand binds to the protein. Protoheme−CO shows somewhat higher values around 10^{11} s^{-1} (Miers et al., 1991). This difference in pre-exponentials suggests an entropic control of the ligand binding reaction by the protein. In AzNO, we measured a pre-exponential of $10^{8.3}$ s^{-1}. With $\nu \approx 10^{12}$ s^{-1}, the pre-exponential of AzNO rebinding reflects a decrease in the number of states by almost a factor of 10^4 in the transition state compared with the dissociated state B. To our surprise, the majority population I in HaNO has a very large pre-exponential of $10^{12.2}$ s^{-1}, implying that there is no significant entropy bottleneck for recombination. By contrast, the pre-exponential of the minority population II is $10^{8.9}$ s^{-1}, which is more in line with the Az and Mb data. The vastly different rebinding barriers and pre-exponentials in the two HaNO species imply significant structural differences at the active site.

The bimolecular recombination in AzNO and HaNO is exponential. The Arrhenius plot of the overall rate coefficients λ_S between 200 and 260 K is linear. From the slope, an enthalpy H_S of 62 kJ/mol for AzNO and 74 kJ/mol for HaNO can be determined. The temperature dependence is similar to that of the bimolecular recombination in protoheme−CO and MbCO in glycerol/water solutions. Moreover, the temperature dependence of the solvent viscosity falls in the same range of enthalpies. Consequently, we conclude that the bimolecular rate coefficient in this temperature region is strongly affected by the dynamics of the viscous solvent.

Hierarchy of Conformational Substates. A hierarchical arrangement of the substates in the conformational energy landscape of MbCO has been proposed (Ansari et al., 1987; Frauenfelder et al., 1994). On the highest tier (CS0), a few taxonomic substates exist, separated by high-energy barriers. These substates can be distinguished by different stretch frequencies of the bound CO. Within the CS0 substates, a large number of conformational substates of tier 1 (CS1) exist with lower barriers. The existence of lower tiers (CS2 and CS3) is also suggested by the experimental data. Switching between the CS0 substates provides an efficient control mechanism of protein function.

The hierarchical arrangement of the CS may reflect the hierarchy of structural features in proteins. Strong covalent bonds establish the primary sequence, hydrogen bonds maintain the secondary structure, and only relatively weak forces like van der Waals forces and additional hydrogen bonds determine the folding into the three-dimensional structure. Since all proteins obey the same design principles, the hierarchical arrangement should apply to proteins in general.

Infrared spectroscopy was essential for the identification of the CS0 substates. While the kinetic separation of the CS0 in MbCO is insufficient in the visible spectrum, flash

photolysis with monitoring in the CO stretch bands showed that the three different CS0 substates rebind with different rates (Young et al., 1991). In the experiments on HaNO reported here, we have observed two kinetically very distinct populations I and II that maintain a fixed population ratio at low temperature, representing two noninterconverting populations, which are analogous to the CS0 substates in MbCO. The pronounced kinetic separation of process II from process I arises from the combined effect of higher rebinding barriers (see Figure 5) and the pre-exponential, which is 3 orders of magnitude smaller for process II.

In their EPR studies of the His117Gly mutant of azurin, den Blaauwen and Canters (1993) noticed that the $A_{\|}$ and $g_{\|}$ values clustered in three distinct regions in the Vänngård–Peisach–Blumberg plot. They speculated that the protein prefers a few discrete structures of the metal site instead of a continuous variation. This view is in agreement with our findings in MbCO and HaNO, where a few taxonomic substates with markedly different properties exist.

Within each taxonomic substate, a large number of substates in lower tiers exist with slightly different structures and functional properties, as evident from the nonexponential rebinding. This observation agrees with EPR studies of Brill and collaborators (Brill, 1978; Aqualino et al., 1991). The EPR spectrum at cryogenic temperatures was explained with a Gaussian distribution of the tetrahedral angle of the lobes of the ground state orbital of the cupric site. The fact that the cupredoxins provide a rather rigid polypeptide environment for the copper ion does not exclude structural heterogeneity.

While evidence is lacking so far for a biological function associated with NO binding to blue copper sites, we have shown that this reaction is a useful tool for obtaining important information about the conformational energy landscape in β-sheet proteins. Detailed investigations of ligand binding in myoglobin and other heme proteins have led to models and concepts regarding conformational heterogeneity and dynamics that were presumed to be relevant for proteins in general. Our studies with cupredoxins imply that these concepts can indeed be extended to other classes of proteins with completely different secondary and active site structure.

ACKNOWLEDGMENT

We thank K. Chu, C. Eng, B. McMahon, J. Müller, and R. D. Young for their collaboration and H. Frauenfelder for helpful comments on the manuscript.

REFERENCES

Adman, E. T. (1985) in *Topics in Molecular and Structural Biology: Metalloproteins* (Harrison, P., Ed.) Vol. 1, pp 1–42, Macmillan, New York.

Adman, E. T. (1991) *Adv. Protein Chem. 42*, 145.

Agmon, N., & Hopfield, J. J. (1983) *J. Chem. Phys. 79*, 2042.

Alberding, N., Austin, R. H., Chan, S. S., Eisenstein, L., Frauenfelder, H., Gunsalus, I. C., & Nordlund, T. M. (1976) *J. Chem. Phys. 65*, 4701–4711.

Ansari, A., Berendzen, J., Bowne, S. F., Frauenfelder, H., Iben, I. E. T., Sauke, T. B., Shyamsunder, E., & Young, R. D. (1985) *Proc. Natl. Acad. Sci. U.S.A. 85*, 5000.

Ansari, A., Berendzen, J., Braunstein, D., Cowen, B. R., Frauenfelder, H., Hong, M. K., Iben, I. E. T., Johnson, J. B., Ormos, P., Sauke, T. B., Scholl, R., Schulte, A., Steinbach, P. J., Vittitow, J., & Young, R. D. (1987) *Biophys. Chem. 26*, 337.

Aqualino, A., Brill, A. S., Bryce, G. F., & Gerstman, B. S. (1991) *Phys. Rev. A 44*, 5257.

Austin, R. H., Beeson, K. W., Eisenstein, L., Frauenfelder, H., & Gunsalus, I. C. (1975) *Biochemistry 14*, 5355.

Berendzen, J., & Braunstein, D. (1990) *Proc. Natl. Acad. Sci. U.S.A. 87*, 1.

Berendzen, J., Frauenfelder, H., Sauke, T., & Scholl, R. (1989) *Bull. Am. Phys. Soc. 34*, 880a (abstract).

Brill, A. S. (1978) *Biophys. J. 22*, 139.

Campbell, B. F., Chance, M. R., & Friedman, J. M. (1987) *Science 238*, 373.

Corin, A. F., & Gould, I. R. (1989) *Photochem. Photobiol. 50*, 413.

den Blaauwen, T., & Canters, G. W. (1993) *J. Am. Chem. Soc. 115*, 1121.

den Blaauwen, T., van de Kamp, M., & Canters, G. W. (1991) *J. Am. Chem. Soc. 113*, 5050.

den Blaauwen, T., Hoitink, C. W. G., Canters, G. W., Han, J., Loehr, T. M., & Sanders-Loehr, J. (1993) *Biochemistry 32*, 12455.

Ehrenstein, D., & Nienhaus, G. U. (1992) *Proc. Natl. Acad. Sci. U.S.A. 89*, 9681.

Frauenfelder, H., & Wolynes, P. G. (1985) *Science 229*, 337.

Frauenfelder, H., Petsko, G. A., & Tsernoglou, D. (1978) *Nature (London) 280*, 558.

Frauenfelder, H., Nienhaus, G. U., & Young, R. D. (1994) in *Disorder Effects on Relaxation Processes* (Blumen, A., & Richert, R., Eds.) pp 591–614, Springer Verlag, Berlin.

Garrett, T. P. J., Clingerleffer, D. J., Guss, J. M., Rogers, S. J., & Freeman, H. C. (1984) *J. Biol. Chem. 259*, 2822.

Gorren, A. C. F., de Boer, E., & Wever, R. (1987) *Biochim. Biophys. Acta 916*, 38.

Gray, H. B., & Malmström, B. G. (1983) *Comments Inorg. Chem. 2*, 203.

Gray, H. B., & Solomon, E. I. (1981) in *Copper Proteins* (Spiro, T. G., Ed.) pp 1–39, Wiley, New York.

Han, J., Loehr, T. M., Lu, Y., Valentine, J. S., Averill, B. A., & Sanders-Loehr, J. (1993) *J. Am. Chem. Soc. 115*, 4256.

Hartmann, H., Parak, F., Steigemann, W., Petsko, G. A., Ringe Ponzi, D., & Frauenfelder, H. (1982) *Proc. Natl. Acad. Sci. U.S.A. 79*, 4967.

Keyes, M. H., Falley, M., & Lumry, R. (1971) *J. Am. Chem. Soc. 93*, 2035.

Lu, Y., LaCroix, L. B., Lowery, M. D., Solomon, E. I., Bender, C. J., Peisach, J., Roe, J. A., Gralla, E. B., & Valentine, J. S. (1993) *J. Am. Chem. Soc. 115*, 5907.

Martin, C. T., Morse, R. H., Kanne, R. M., Gray, H. B., Malmström, B. G., & Chan, S. I. (1981) *Biochemistry 20*, 5147.

Mattar, S., Scharf, B., Kent, S., Rodewald, K., Oesterhelt, D., & Engelhard, M. (1994) *J. Biol. Chem. 269*, 14939.

Miers, J. B., Postlewaite, J. C., Zyung, T., Chen, S., Roemig, G. R., Wen, X., & Dlott, D. D. (1990) *J. Chem. Phys. 93*, 8771.

Mizoguchi, T. J., Di Bilio, A. J., Gray, H. B., & Richards, J. H. (1992) *J. Am. Chem. Soc. 114*, 10076.

Mourant, J. R., Braunstein, D. P., Chu, K., Frauenfelder, H., & Nienhaus, G. U. (1993) *Biophys. J. 65*, 1496.

Murphy, L. M., Strange, R. W., Karlsson, B. G., Lundberg, L. G., Pascher, T., Reinhammar, B., & Hasnain, S. S. (1993) *Jpn. J. Appl. Phys. 32*, 561.

Nar, H., Huber, R., Messerschmidt, A., Filipou, A. C., Barth, M., Jaquinod, M., van de Kamp, M., & Canters, G. W. (1992) *Eur. J. Biochem. 205*, 1123.

Ormos, P., Ansari, A., Braunstein, D., Cowen, B. R., Frauenfelder, H., Hong, M. K., Iben, I. E. T., Sauke, T. B., Steinbach, P. J., & Young, R. D. (1990) *Biophys. J. 57*, 191.

Parak, F., Hartmann, H., & Nienhaus, G. U. (1987) in *Protein Structure; Molecular and Electronic Reactivity* (Austin, R., Buhks, E., Chance, B., De Vault, D., Dutton, P. L., Frauenfelder, H., & Goldanskii, V. I., Eds.) pp 65–81, Springer, New York.

Romero, A., Hoitink, C. W. G., Nar, H., Huber, R., Messerschmidt, A., & Canters, G. W. (1993) *J. Mol. Biol. 229*, 1007.

Sanders-Loehr, J. (1993) in *Bioinorganic Chemistry of Copper* (Karlin, K. D., & Tyeklár, Z., Eds.) pp 51–63, Chapman & Hall, New York.

Scharf, B., & Engelhard, M. (1993) *Biochemistry 32*, 12894.

Shepard, W. E. B., Anderson, B. F., Lewandoski, D. A., Norris, G. E., & Baker, E. N. (1990) *J. Am. Chem. Soc. 112*, 7817.

Solomon, E. I., & Lowery, M. D. (1993) *Science 259*, 1575.
Šrajer, V., Reinisch, L., & Champion, P. M. (1988) *J. Am. Chem. Soc. 110*, 6656.
Stein, D. L. (1985) *Proc. Natl. Acad. Sci. U.S.A. 82*, 3670.
Steinbach, P. J., Ansari, A., Berendzen, J., Braunstein, D., Chu, K., Cowen, B. R., Ehrenstein, D., Frauenfelder, H., Johnson, B., Lamb, D. C., Luck, S., Mourant, J. R., Nienhaus, G. U., Ormos, P., Philipp, R., Xie, A., & Young, R. D. (1991) *Biochemistry 30*, 3988.
Steinbach, P. J., Chu, K., Frauenfelder, H., Johnson, J. B., Lamb, D. C., Nienhaus, G. U., Sauke, T. B., & Young, R. D. (1992) *Biophys. J. 61*, 235.
Suzuki, S., Yoshimura, T., Kohzuma, T., Shidara, S., Masuko, M., Sakurai, T., & Iwasaki, H. (1989) *Biochem. Biophys. Res. Commun. 164*, 1366.
Sykes, A. G. (1991) in *Advances in Inorganic Chemistry*, Vol. 36, pp 377−408, Academic Press, New York.
van Leeuwen, F. X. R., & van Gelder, B. F. (1978) *Eur. J. Biochem. 87*, 305.
van Leeuwen, F. X. R., Wever, R., van Gelder, B. F., Avigliano, L., & Mondovi, B. (1975) *Biochim. Biophys. Acta 403*, 285.
Wever, R., van Leeuwen, F. X. R., & Van Gelder, B. F. (1973) *Biochim. Biophys. Acta 302*, 236.
Williams, R. J. P. (1971) *Inorg. Chim. Acta, Rev. 5*, 137.
Young, R. D., & Bowne, S. F. (1984) *J. Chem. Phys. 81*, 3730.
Young, R. D., Frauenfelder, H., Johnson, J. B., Lamb, D. C., Nienhaus, G. U., Philipp, R., & Scholl, R. (1991) *Chem. Phys. 158*, 315.

BI950403P